

LANE 2012

# Ultrafast lasers improve the efficiency of CIS thin film solar cells

Gerhard Heise<sup>a,\*</sup>, Andreas Heiss<sup>b</sup>, Helmut Vogt<sup>b</sup>, Heinz P. Huber<sup>a</sup>

<sup>a</sup>Lasercenter of the Munich University of Applied Sciences (MUAS), Department of Precision- and Microengineering, Engineering Physics, Lothstraße 34, D-80335 Munich, Germany

<sup>b</sup>AVANCIS GmbH & Co. KG, Otto-Hahn-Ring 6, D-81739 Munich, Germany

---

## Abstract

CIS (Cu(In,Ga)(S,Se)<sub>2</sub>) thin film solar cells show a high potential to achieve the efficiencies of Si wafer-based solar cells. The commonly applied patterning processes for the integrated interconnects are based on nanosecond laser ablation and mechanical scribing. Both methods introduce damages on the thin films by thermal effects and mechanical forces. By picosecond laser processing we realized all three patterning steps to the monolithic thin films CIS modules, namely the separation of the molybdenum back electrode, the absorber and the ZnO front electrode (P1, P2 and P3 respectively). We achieved an efficiency of 14.7% for 300 x 300 mm<sup>2</sup> modules.

© 2012 Published by Elsevier B.V. Selection and/or review under responsibility of Bayerisches Laserzentrum GmbH  
Open access under [CC BY-NC-ND license](https://creativecommons.org/licenses/by-nc-nd/4.0/).

*Keywords:* Laser ablation; Ultrafast laser; Picosecond laser; Monolithic interconnection; Selective structuring; thin film; solar cell; CIS

---

## 1. Introduction

Thin film solar modules can be manufactured in an economical in-line process, consuming considerably less materials than solar cells based on bulk absorbers. Especially CIS (Cu(In,Ga)(S,Se)<sub>2</sub>) thin film solar cells are of general interest due to their high module efficiency exceeding 15 % on 300 x 300 mm<sup>2</sup> test modules [1-4]. A CIS thin film solar cell consists of the CIS p-type absorber layer sandwiched between the metallic p-contact and the transparent n-contact, see Figure 1. In order to minimize ohmic losses due to the limited conductivity of the transparent front electrode, the large area is

---

\* Corresponding author. Tel.: +49-89-1265-3676 ; fax: +49-89-1265-1603 .  
E-mail address: [gerhard.heise@hm.edu](mailto:gerhard.heise@hm.edu) .

divided into smaller cells which are electrically connected in series [5, 6]. A typical cell size is about 5 mm, at his distance the monolithical interconnect region repeats.

In production, patterning processes for these integrated interconnects between the cells are either based on nanosecond laser ablation [7, 8] or mechanical scribing [9, 10]. Both processes introduce damage to the thin films by mechanical forces or thermal effects. The structured lines are irregular and force a large safety distance of more than 300  $\mu\text{m}$ , see Figure 5, right. This dead area is not available to generate electrical power from sunlight. Furthermore, the scribing speed achievable mechanically is limited to about 1 m/s and the scribing needles have a limited lifetime generating considerable cost for maintenance. Therefore, it is desirable and cost effective to replace the mechanical processes by the precise high speed laser processes without wear presented in this article.

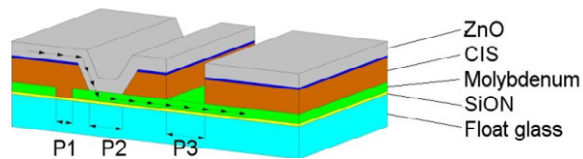


Fig. 1. Schematic cross-section of the serial interconnect region of a CIS thin film solar cell. The glass substrate is carrying a below 1  $\mu\text{m}$  thick molybdenum layer followed by ca. 1-3  $\mu\text{m}$  thick CIS layer covered by a 1 – 2  $\mu\text{m}$  ZnO layer. The regions labeled with P1, P2 and P3 are indicating the structuring patterns for the monolithic serial connection. The chain of arrows is displaying the path of the electron flow

## 2. Material and Methods

Samples consisting of 3 mm thick float glass substrates with a size of 300 x 300  $\text{mm}^2$  are prepared at AVANCIS in the Munich R&D pilot line [3]. The P1 structuring experiments to achieve a galvanic separation of the p-contact were performed on below 1  $\mu\text{m}$  thick molybdenum films. Between the glass substrate and the molybdenum there is a thin silicon nitride barrier layer which must not be damaged by the ablation process. In the pattern 2 (P2) ablation process, the isolating CIS layer (1- 3  $\mu\text{m}$  thickness) has to be removed completely to enable a good contact of the molybdenum layer to the ZnO layer being deposited in a later process step. The P3 separation of the n-contact by mechanical scribing removes the complete combined ZnO/CIS layer on top of the Mo. With ps laser ablation it is advantageous to ablate only the highly conductive transparent ZnO layer (1 -2  $\mu\text{m}$ ) on top of the CIS because a higher processing speed can be achieved and a lower thermal impact is inflicted upon the remaining layers.

Using an ultrafast laser (High Q Laser picoREGEN UC-30000) at a wavelength 1064 nm with a pulse duration of about 10 ps and a maximum power of 30 W, we realized all three patterning steps successfully as demonstrated in the left part of Figure 5. Most processes were performed with a laser spot diameter of 40  $\mu\text{m}$  ( $1/e^2$ ), using an f-theta optics with a focal length of 250 mm.

## 3. Results

### 3.1. P1 patterning of molybdenum

The molybdenum is ablated (P1 pattern) by irradiating the metal layer from the glass side. This lift-off process utilizes the lasers energy very efficiently, allowing a high speed structuring process[11]. Trenches have been scribed with repetition rates between 10 and 950 kHz. The ablation threshold remained nearly independent of repetition rate, indicating a single pulse process with no interaction between adjacent

spots. We achieved processing speeds up to 15 m/s, limited by the speed of our scanner system. The directly induced ablation process is highly selective between Mo and the silicon nitride barrier [8, 10, 12]. P1 lines scribed with picosecond lasers are demonstrated in the microphotographs of Figure 2 showing a P1 trench (left) and the intersection of a P1 trench and the isocut line for edge isolation. Micro cracks below and adjacent to the P1 trench are hardly present and the electrical isolation of P1 is increased compared to ns laser P1.

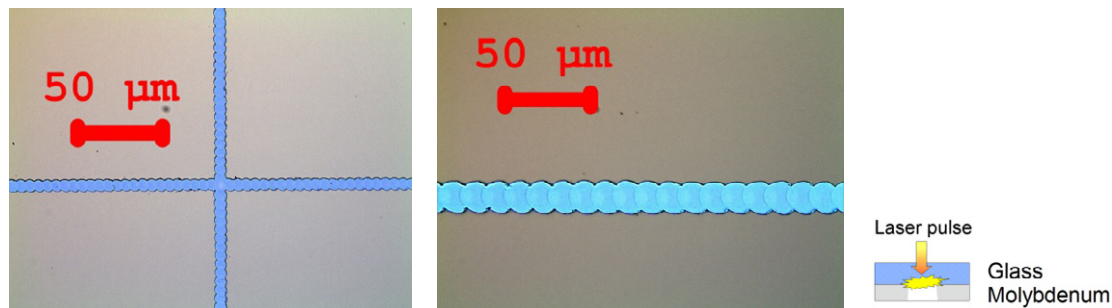


Fig. 2. Patterning of molybdenum from the glass side with 10 ps pulses at 1064 nm (P1 process, schematic sketch on the right). Microscopic images with front- and backside illumination, the light blue region represents the exposed barrier layer. (a) single P1 trench with  $\sim 30\%$  pulse overlap; (b) intersection of P1 line with isocut line, demonstrating that the barrier remains intact even with double exposure

### 3.2. P2 patterning of CIS absorber

Ablation thresholds using a 10 ps laser at 1064 nm for Mo front and back side, CIS on Mo, and ZnO on CIS have been published elsewhere [13]. They have been derived from measurements of the ablation spot diameter as a function of laser fluence, which has been varied typically between 0.1 and 10 J/cm<sup>2</sup> in 10 to 20 steps. Figure 3 left shows as an example a graph to determine the ablation threshold of CIS (P2). The fluence at the intersection of the fitted straight lines at a diameter of zero, 0.14 J/cm<sup>2</sup>, is called the threshold value for the corresponding process. Starting from the single pulse ablation threshold, the parameters to scribe trenches are evaluated. Scribing speeds up to 4 m/s could be realized.

The right side of Figure 3 shows an SEM micrograph of a P2 scribe written with direct ablation and a pulse overlap exceeding 20 pulses per position. At the bottom of the trenches the molybdenum is exposed and no residual CIS can be detected. The ripples in the Mo film are typical for an ablation with linear polarized light. Their amplitude is reduced considerably when the trenches are scribed with circular polarized light. The about 3 μm wide heat affected zone with an obviously fused rim does not affect the performance of the P2 trenches [14].

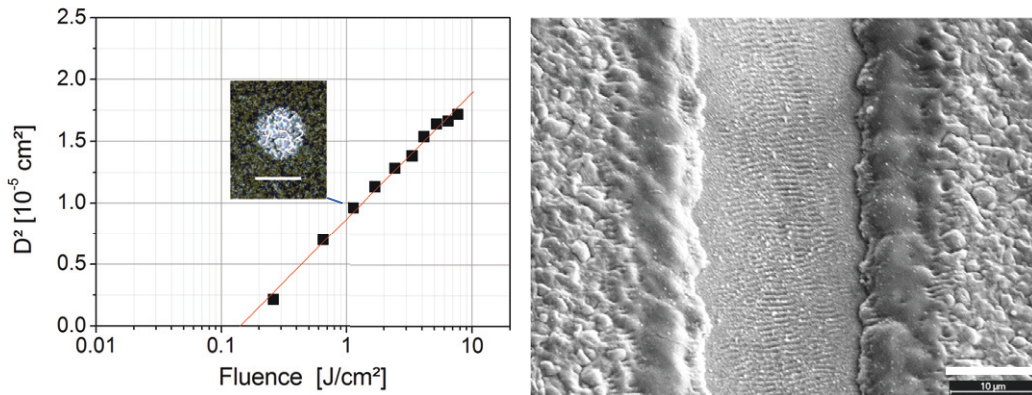


Fig. 3. (a) ablation experiments of CIS with a 10 ps laser pulse at 1064 nm. Spot radius squared ( $D^2$ ) vs. laser fluence. The symbols (■) correspond to measured values. The inset shows a microscopic image of a typical ablated spot; (b) SEM Micrograph of P2 trench demonstrating the clean and intact molybdenum layer at the bottom. The ripples in the molybdenum are related to the linear polarization of the laser. Scale bar length is 10 μm

To assess the quality of the P2 grooves, we determined the contact resistance of the ZnO/Mo interface in the P2 groove by an interconnect test structures (ITS) [14]. The ITS design and principle is posed in Figure 4, left. Each cell contains two P2 trenches separated by one P1 trench; the distance  $b$  between the two P2 trenches of one cell varies. Electrical current is injected through the molybdenum layer and flows from the first P2 trench through the ZnO layer to the second P2 trench.

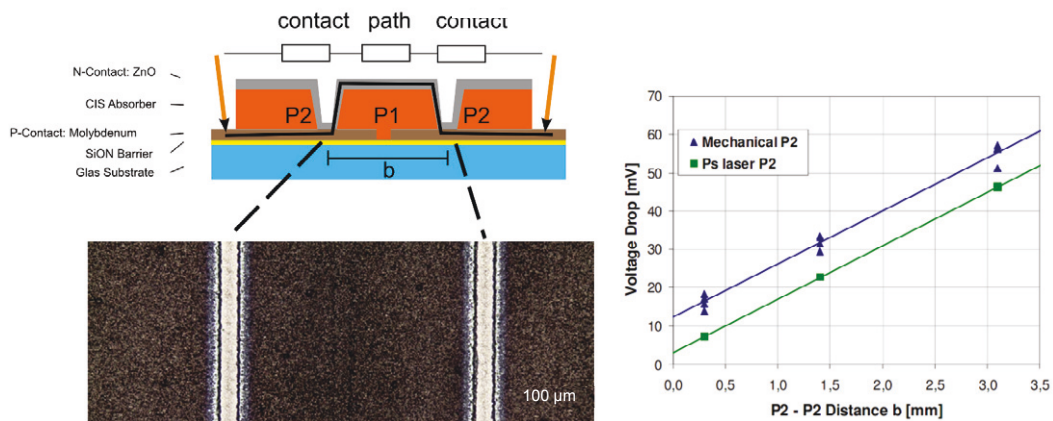


Fig. 4. (a) schematic (top) and microscopic image (bottom) of ITS structure. P2 lines written with varying distances  $b$  to evaluate the contact resistance of the Mo-ZnO interface. The black line marks the current flow; (b) voltage drop at a fixed current as function of P2 trench separation for trenches applied by mechanical scribing (▲ blue triangles and line) and for laser ablated trenches (■ green squares and line). The voltage drop for the laser ablated trenches is obviously smaller than that for mechanically generated trenches

The voltage drop between the contact needles depends on both, the resistance of the ZnO layer, and the contact resistance of the Mo/ZnO interface. As the length  $b$  of the ZnO path is varied, the contact resistance can be extrapolated for  $b = 0$ . This test was carried out on samples with mechanical P2 scribes

as the reference and for P2 scribed with ps lasers. The measured voltage drop is plotted versus the P2-P2 trench distance, see Figure 4, right. The slope of the linear fit is an indicator of the sheet resistance of the ZnO layer, and the intersection point of the y-axis indicates the voltage drop at the P2 trench. The voltage drop for mechanical structuring was about 12 mV, whereas the voltage drop for both ps laser processes was only about 3-4 mV for equal electrical current. Thus, the ps laser process provides a better contacting between Mo and ZnO.

### 3.3. P3 patterning of zinc oxide

The transparent front contact can be removed with an indirect induced laser ablation process with low pulse overlap and no interaction between the single pulses. In contrast to P1 here the underlying CIS is the absorbing partner and the ZnO is the transparent partner. The laser ablation of the ZnO is indirectly induced by the underlying CIS [15]. A scribing speed of up to 15 m/s was achieved, limited by the scanner. A sample picture of a laser P3 scribe is shown in Figure 5, left. Laser patterning of the front electrode still bears some remaining risks of shunting in P3, most likely by the generation of binary phases in the absorber [16].

### 3.4. Solar cell performance

As the P1/P2/P3 patterning zone does not contribute to the solar module efficiency, a reduction of the dead area is one important measure to enhance solar module efficiency. State of the art mechanical patterning of P2 and P3 causes chipping. Especially P2 chipping limits reduction of the dead area as P2 chippings crossing P1 causes shunts between front and back electrode. Furthermore mechanical P3 does not work equally effective on areas being affected by mechanical P2 chipping where there is a direct deposition of ZnO on Mo. Figure 5 shows the direct comparison of a monolithical interconnect region scribed mechanically (right side) and scribed with picosecond lasers (left side). The dead area is nearly by a factor of 2 with no chipping. 300 x 300 mm<sup>2</sup> CIS solar module with an integrated serial interconnection totally performed by picosecond laser patterning processes achieved an aperture area efficiency of 14.7%

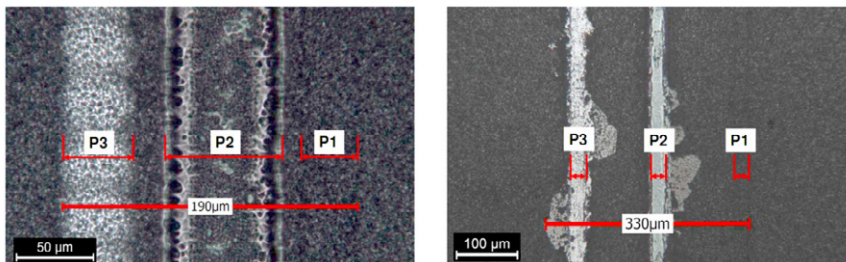


Fig. 5. (a) optical micrographs of patterning trenches as applied for the 14.7%-module in comparison to (b) the previously used ns laser P1 and mechanical P2/P3

## 4. Conclusion

Picosecond laser structuring of the monolithical serial interconnection of CIS was performed for the direct induced ablation of molybdenum on glass (P1), the direct ablation of CIS on Mo (P2) and the indirectly induced ablation of ZnO on CIS (P3). It was shown, that picosecond laser structuring of the P2

scribes results in a reduced contact resistance. The very well defined ablation trenches allow to reduce dead area of the monolithical interconnect. Both increases the efficiency of the solar cell to a maximum value of 14.7%

## Acknowledgements

This work was funded by the German Federal Ministry for the Environment, Nature Conservation and Nuclear Safety within the project "SECIS" under grant No. 0325043A/B. We thank our colleagues from Munich University of applied Sciences: Helmut Herberg and Michael Kaiser for the help with confocal image profiling and Ursula Koch and Constanze Eulenkamp for SEM support.

## References

- [1] T. Dalibor, S. Jost, H. Vogt, A. Heiß, S. Visbeck, T. Happ, J. Palm, A. Avellán, T. Niesen and F. Karg, "Towards Module Efficiencies of 16% with an Improved CIGSSe Device Design," in 26th European Photovoltaic Solar Energy Conference and Exhibition Hamburg, 2011, pp. 2407-2411.
- [2] M. A. Green, K. Emery, Y. Hishikawa, W. Warta and E. D. Dunlop, "Solar cell efficiency tables (Version 38)", *Progress in Photovoltaics: Research and Applications*, vol. 19, pp. 565-572, 2011.
- [3] V. Probst, J. Palm, S. Visbeck, T. Niesen, R. Tölle, A. Lerchenberger, M. Wendl, H. Vogt, H. Calwer, W. Stetter and F. Karg, "New developments in Cu(In,Ga)(S, Se)<sub>2</sub> thin film modules formed by rapid thermal processing of stacked elemental layers", *Solar Energy Materials and Solar Cells*, vol. 90, pp. 3115-3123, 2006// 2006.
- [4] I. Repins, M. A. Contreras, B. Egaas, C. DeHart, J. Scharf, C. L. Perkins, B. To and R. Noufi, "19.9%-efficient ZnO/CdS/CuInGaSe<sub>2</sub> solar cell with 81.2% fill factor", *Progress in Photovoltaics: Research and Applications*, vol. 16, pp. 235-239, 2008.
- [5] B. Dimmler, M. Powalla and R. Schaeffler, "CIS solar modules: Pilot production at Wuerth Solar," in Conference Record of the IEEE Photovoltaic Specialists Conference, Lake Buena Vista, FL, 2005, pp. 189-194.
- [6] W. J. Biter, "Photovoltaic device and method of making same," USA Patent US4042418 (A), 1977-08-16, 1977.
- [7] A. D. Compaan, I. Matulionis and S. Nakade, "Laser scribing of polycrystalline thin films", *Optics and Lasers in Engineering*, vol. 34, pp. 15-45, 2000.
- [8] C. Molpeceres, S. Lauzurica, J. L. Ocana, J. J. Gandia, L. Urbina and J. Carabe, "Microprocessing of ITO and a-Si thin films using ns laser sources", *Journal of Micromechanics and Microengineering*, vol. 15, pp. 1271-1278, 2005.
- [9] B. Dimmler and H. W. Schock, "Scaling-up of CIS technology for thin-film solar modules", *Progress in Photovoltaics: Research and Applications*, vol. 4, pp. 425-433, 1996// 1996.
- [10] V. Probst, F. Karg, J. Rimmasch, W. Riedl, W. Stetter, H. Harms and O. Eibl, "Advanced stacked elemental layer process for Cu(InGa)Se<sub>2</sub> thin film photovoltaic devices," in Materials Research Society Symposium - Proceedings, San Francisco, CA, USA, 1996, pp. 165-176.
- [11] G. Heise, M. Englmaier, C. Hellwig, T. Kuznicki, S. Sarrach and H. Huber, "Laser ablation of thin molybdenum films on transparent substrates at low fluences", *Applied Physics A: Materials Science and Processing*, vol. 102, pp. 173-178, 2011.
- [12] G. Heise, M. Domke, J. Konrad, F. Pavic, M. Schmidt, H. Vogt, A. Heiss, J. Palm and H. P. Huber, "Monolithical Serial Interconnects of large CIS Solar Cells with Picosecond Laser Pulses", *Physics Procedia*, vol. 12, pp. 149-155, 2011.

- [13] G. Heise, A. Heiss, C. Hellwig, T. Kuznicki, H. Vogt, J. Palm and H. P. Huber, "Optimization of picosecond laser structuring for the monolithic serial interconnection of CIS solar cells", *Progress in Photovoltaics: Research and Applications*, 2012.
- [14] P. O. Westin, U. Zimmermann and M. Edoff, "Laser patterning of P2 interconnect via in thin-film CIGS PV modules", *Solar Energy Materials and Solar Cells*, vol. 92, pp. 1230-1235, 2008.
- [15] G. Heise, M. Dickmann, M. Domke, A. Heiss, T. Kuznicki, J. Palm, I. Richter, H. Vogt and H. Huber, "Investigation of the ablation of zinc oxide thin films on copper–indium–selenide layers by ps laser pulses", *Applied Physics A: Materials Science and Processing*, vol. 104, pp. 387-393, 2011 2011.
- [16] H. Vogt, A. Heiss, J. Palm, F. Karg, H. P. Huber and G. Heise, "All Laser Patterning Serial Interconnection for Highly Efficient CIGSSe Modules," in *26th EUPVSEC, Hamburg, 2011*, p. 3DV.2.9.